Evolution of the coefficient of lateral earth pressure at rest with interparticle friction: a numerical study

Hoang C Nguyen[1*]

[1]Former PhD student, Department of Civil and Environmental Engineering, Imperial College London, London, UK

Abstract. The grain-scale nature of evolution of the coefficient of lateral earth pressure at rest (K_0) with interparticle friction (μ_p) is poorly understood. This study aims to use discrete element method simulations of vertical one-dimensional compression on both face centred cubic (FCC) samples and random monodisperse (RM) samples to link K_0 and μ_p, and the results show that K_0 increases with reductions in interparticle friction. Although K_0 is dependent upon the sample density, patterns of evolutions with strain levels are likely to be unchanged with initial confining pressures. The stress-induced fabric becomes more anisotropic for samples with high values of the interparticle friction. The percentage of particles with a high value of the normal contact force increases with increasing strain levels as the interparticle friction increases in the simulations.

1 Introduction

Particulate discrete element modelling (DEM) is now well established and provides a wonderful research tool for many branches of engineering science in general, and in geomechanics in particular. This method was proposed in the late 1970s [1] and the steady increase in the number of DEM-related publications published each year show the potential of this numerical method [2]. For geomechanics studies, particulate DEM is relatively simple in terms of input parameters but effective in capturing the key elements of soil behaviour. Numerical DEM analyses allow geomechanics researchers to understand what happens at the particle scale which provides a useful explanation of the overall responses. As outlined in [2], two main motivations for DEM models lie in: (i) link between micro-scale interactions and macro-scale response; and (ii) analysis of large displacement problems in geomechanics. Use of a modified version of the open-source code, Granular LAMMPS [3] allows the highly complex behaviour of granular materials to be successfully captured. Not only can the boundary condition be easily mimicked the conditions that earth pressure is at rest, but micro-scale data gives more insights into grain-scale mechanisms underlying the evolution of K_0 with the conditions that allow particle slide each other at contacts (i.e. μ_p). Several 1D compression tests were performed, allow the link between K_0 and μ_p to be explored. It is usual practice to relate K_0 to the effective friction angle of soil, ϕ' as $K_0 = 1 - sin\phi'$ [4]. Herein the ratio of the ratio of horizontal effective stress, σ'_h to vertical effective stress, σ'_v is used to quantify evolution of K_0 and strain levels due to varying μ_p.

2 DEM simulations

Simulations of 1D compression tests were performed on both the FCC samples and the RM samples using a modified version of the granular LAMMPS code, with a simplified Hertz-Mindlin contact model. The FCC packing consisting of 3,200 spherical particles (the particle diameter of 2.54 mm) that correspond to samples previously used in [5–7] was adopted, while the RM sample was created from an initial cloud of 34, 986 non-contacting monodisperse spherical particles (i.e. the particle diameters ranged from 2.3 to 2.7 mm). Specifically, the input parameters used were shear modulus $G_p = 25 \times 10^9 Pa$, particle Poisson's ratio, $\mu_p = 0.2$, particle density, $\rho_p = 2230\ kg/m^3$ and local damping coefficient, $c_p = 0.01$. The samples were enclosed in the vertical direction by two rigid, planar, horizontal boundaries; periodic boundaries were used in the lateral direction. Herein four values of interparticle frictions which are $\mu_p = 0.05; 0.25; 0.50$ and 0.75 were used to assess the changes in K_0 with strain levels as μ_p is varied. These samples experienced two main processes. In the first step, all samples were isotropically compressed to three different values of confining pressure (i.e. $p_0 = 100; 300$ and $1000kPa$); the void ratio of samples at this stage is denoted as e_0, which is dependently upon the value of μ_p for the RM samples. The second step relates to 1D compressions in which the lateral boundary was fixed, while the top rigid wall was moved at a constant velocity $\dot{\epsilon_z} = 0.1m/s$.

3 DEM results

3.1 Macro response

Macro-scale responses under 1D compression tests were shown in Figure 1 for the FCC packings where the deviator stress increases as μ_p increases. However, the mean

*e-mail: h.nguyen15@imperial.ac.uk

A video is available at https://doi.org/10.48448/ef8f-7540

effective stress, p'_0 is likely to be independent upon on μ_p, most probably due to the very stable configuration (Figure 1 b); however, it is not the case for monodisperse samples where an increase in either μ_p or p'_0 leads to a reduction in initial void ratio (i.e. e_0), agreeing well with numerical results reported in [8]. It is shown in Figure 1 that higher K_0 values were observed for the samples with smaller μ_p. This is also a trend for the RM samples where looser samples experienced higher values of μ_p (Figure 2), along with an increase in the mean effective stress as μ_p increases.

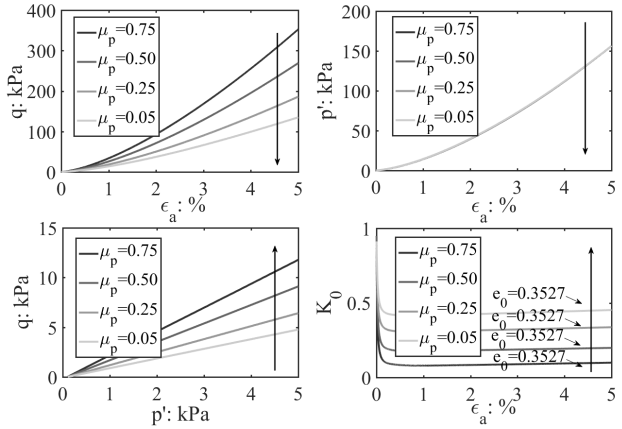

Figure 1. Dependency of macro-scale responses on interparticle friction for the FCC samples that were compressed from p'_0 = 100kPa.

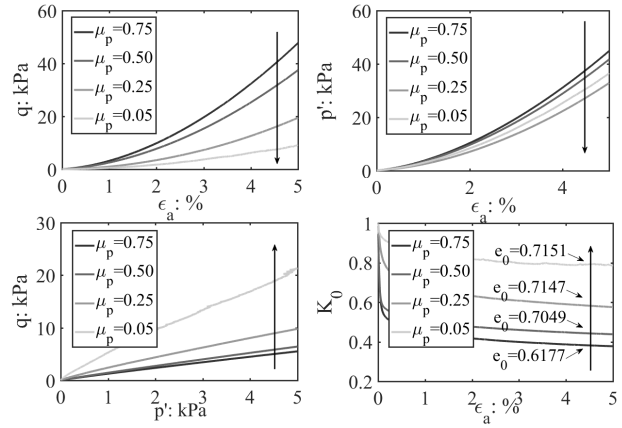

Figure 2. Dependency of macro-scale responses on interparticle friction for the RM samples that were compressed from p'_0 = 100kPa.

Assessments of dependency of K_0 on either the initial void ratio and mean effective confining pressure were made for both samples (Figure 3). It is observed that the K_0 values of both samples are independent upon the initial mean effective pressure. At each stress level, there is a reduction in K_0 as ϵ_a increases, providing a check on the numerical results obtained in [8] who performed 1D simulations on samples with particle size distributions. Interestingly, K_0 continuously reduces over a wide strain range (ϵ_a = 0 : 5%) for the RM samples; however, it is, in contrast to the RM samples, that K_0 is almost unchanged when ϵ_a is larger than 0.1% for the FCC sample.

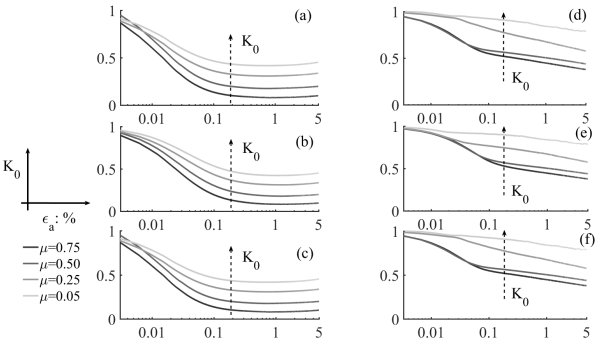

Figure 3. Dependency of macro-scale responses on interparticle friction when samples were compressed from p'_0 = 100kPa: (a) the FCC sample: p'_0 = 100kPa; (b) the FCC sample: p'_0 = 300kPa; (c) the FCC sample: p'_0 = 1000kPa; (d) the RM sample: p'_0 = 100kPa; (e) the RM sample: p'_0 = 300kPa; (f) the RM sample: p'_0 = 1000kPa;.

3.2 Micro-scale analysis

Analyses of particle-scale data extracted from DEM simulations provide additional information on macro-scale responses under one-dimensional compression. The stress-induced fabric anisotropy herein is quantified using: (i) particle orientations; (ii) contact normal orientations. Contact orientations are shown in Figure 4 and Figure 5 using rose diagrams, in which each contact is distributed on the spatial orientation. Specifically, each rose diagram has 18 bins, with angles varying from 0^o to 180^o. The length of each bin represents the number of contacts, with projections onto the xy, xz and yz planes. Referring to Figure 5, the stress-induced fabric is highly sensitive to the strain levels, in which the distribution of contact numbers is isotropic at p'_0 = 1000kPa; however, the fabric anisotropy becomes remarkably for the verticle planes as ϵ_a increases to 5%. In contrast, numbers of contact are more isotropic for the horizontal plane. Along with the contact distributions, evolutions of the normal force at contact were analyzed and shown in Figure 6 and Figure 7. As expected, the degree of anisotropy becomes significantly as μ_p increases for the vertical planes; however, in the horizontal plane, the force distributions remain in an almost isotropic manner due to its fabric isotropy.

Investigations into changes in the coordination number were analysed for both samples (Figure 8a and 8e). While the RM samples experience an increase in N_c as μ_p reduces during 1D compressions, FCC packings show that N_c tends to drop as μ_p increases. In addition, there is no simple link between the friction dissipation and μ_p for both samples (Figure 8b and 8f). However, the pattern of F_n/F_n^{max} (F_n and F_n^{max} are the normal contact force and the maximum normal force at contact respectively) moves to the right as ϵ_a increases, indicating that more particles bear higher magnitudes of the normal force at contacts. Noting that, at p'_0 = 1000kPa, the pattern of F_n/F_n^{max} is almost identical for the RM samples, regardless of the use of different values of μ_p. Changes in the trend of F_n/F_n^{max} for the FCC samples were shown in Figure 8c and 8c where there is no simple correlation between F_n/F_n^{max} and μ_p.

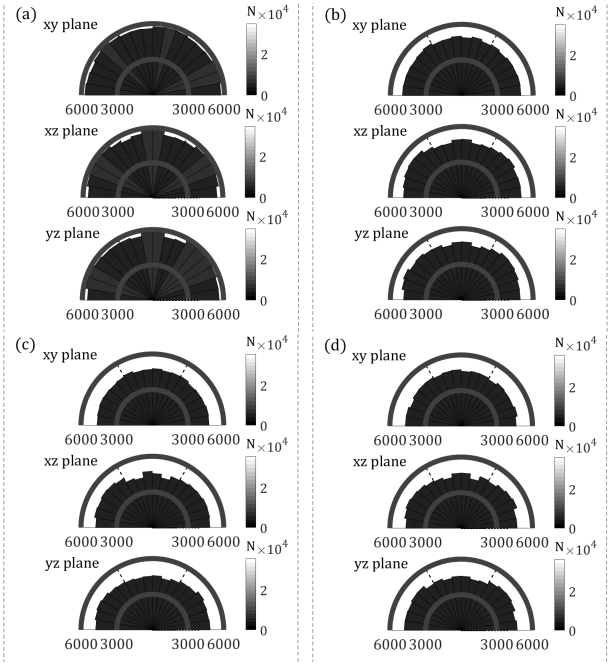

Figure 4. Contact distributions of the RM samples at $p'_0 = 1000kPa$, with projections onto the xy, xz and yz planes, respectively: (a) $\mu_p = 0.05$; (b) $\mu_p = 0.25$; (c) $\mu_p = 0.50$; and (d) $\mu_p = 0.75$.

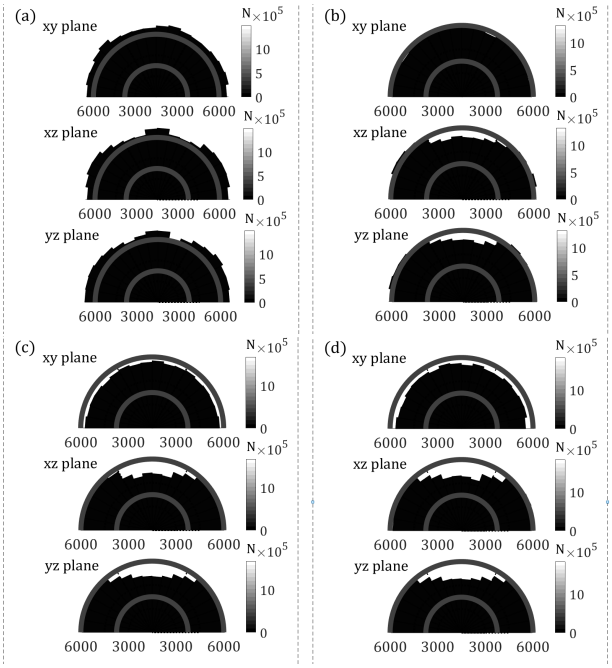

Figure 5. Contact distributions of the RM samples at $\epsilon_a = 0.5\%$, with projections onto the xy, xz and yz planes, respectively: (a) $\mu_p = 0.05$; (b) $\mu_p = 0.25$; (c) $\mu_p = 0.50$; and (d) $\mu_p = 0.75$.

Figure 8i and Figure 8j show the normalised contact force values for the RM samples at $p_0 = 1000kPa$ and at $\epsilon_a = 5\%$. The value of mean normal contact force for the whole sample is denoted as F_n^{mean} and is calculated using micro-scale data at contacts being extracted from DEM simulations. From a particle-scale perspective, the normalised contact force values represent the ability that stress is transmitted through granular materials as noted in [9]. Although the friction value has no influence on the

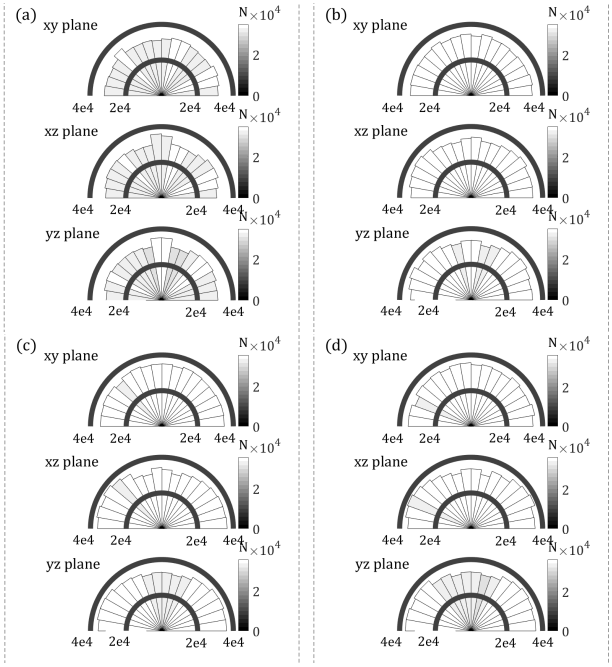

Figure 6. Normal force distributions of the RM samples at $p'_0 = 1000kPa$, with projections onto the xy, xz and yz planes, respectively: (a) $\mu_p = 0.05$; (b) $\mu_p = 0.25$; (c) $\mu_p = 0.50$; and (d) $\mu_p = 0.75$.

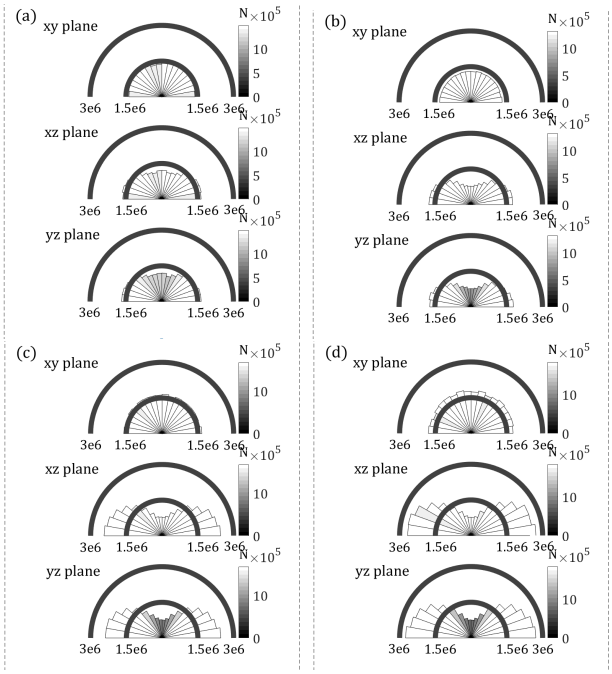

Figure 7. Normal force distributions of the RM samples at $\epsilon_a = 0.5\%$, with projections onto the xy, xz and yz planes, respectively: (a) $\mu_p = 0.05$; (b) $\mu_p = 0.25$; (c) $\mu_p = 0.50$; and (d) $\mu_p = 0.75$.

pattern of normalised contact force, there is an increase in the number of particles that bears higher normal force as the axial strain increases, with the plots of F_n/F_n^{mean} being shifted to the right as shown in Figure 8j. This implies that more chains of highly stressed particles are formed during one-dimensional compression tests, where more stress is transmitted in the vertical planes than in the horizontal plane as previously shown in Figure 6 and Figure 7.

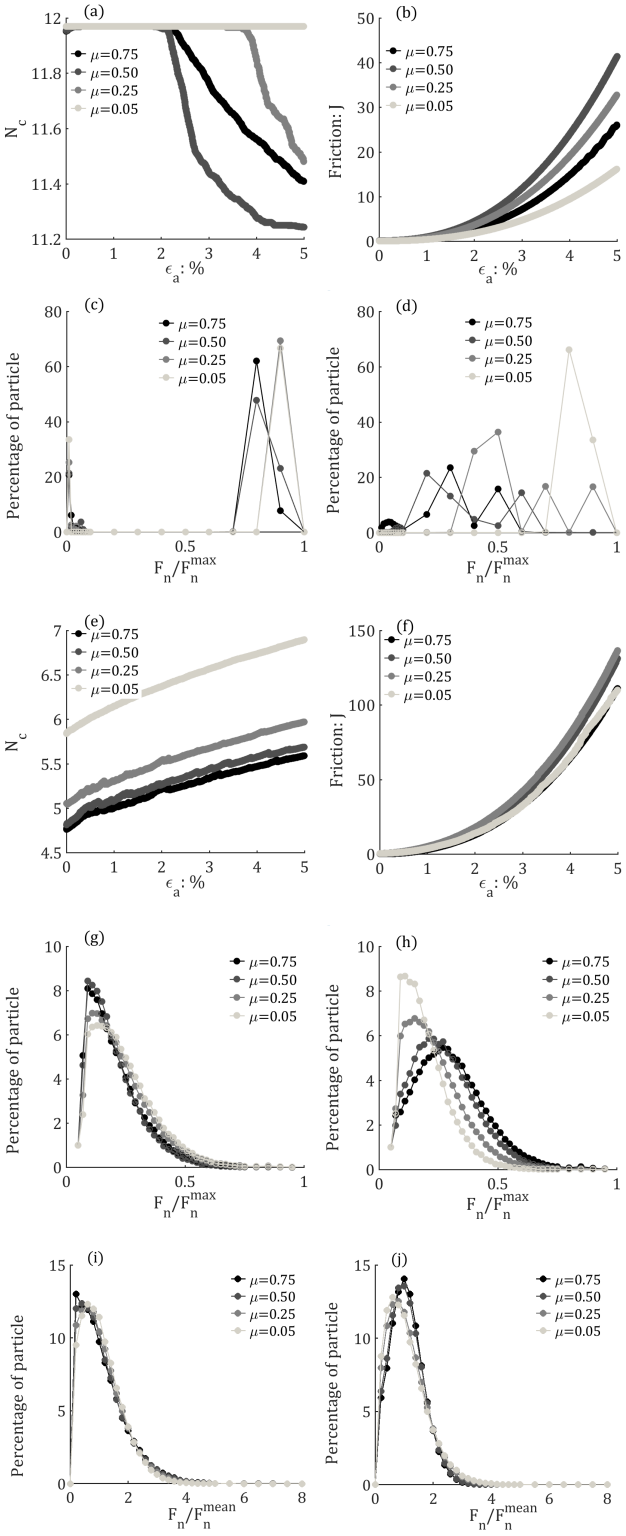

Figure 8. Evolutions of the coordination number and friction dissipation with axial strain: (a) N_c: the FCC sample; (b) friction: the FCC sample; (c) F_n/F_n^{max} at $p'_0 = 1000kPa$: the FCC sample; (d) F_n/F_n^{max} at $\epsilon_a = 5\%$: the FCC sample; (e) N_c: the RM sample; (f) friction: the RM sample; (g) F_n/F_n^{max} at $p'_0 = 1000kPa$: the RM sample; (h) F_n/F_n^{max} at $\epsilon_a = 5\%$: the RM sample; (i) F_n/F_n^{mean} at $p'_0 = 1000kPa$: the RM sample; and (j) F_n/F_n^{mean} at $\epsilon_a = 5\%$: the RM sample.

4 Conclusions

The link between K_0 and μ_p has been described using one-dimensional DEM simulations, arriving at the observation that K_0 decreases as μ_p increases. Although K_0 depends on the sample density and the material fabric, there is no dependency of K_0 on the confining pressure. While the FCC sample experiences a drop in the coordination number as the strain level increases, it is observed that there is a rise in the coordination number for the RM samples. There is no simple link between the friction dissipation and the interparticle friction; however, the coordination number increases with increasing interparticle friction for the randomly monodisperse size sample. The pattern of F_n/F_n^{max} moves to the right as the strain level increases, indicating that more particles bear the high magnitude of the normal contact force. The extent of the strain-induced anisotropy depends on the K_0 value, with higher degree of anisotropy for samples with larger values of the interparticle friction. The results of this study support the prior findings reported in [8] who confirmed that the values of K_0 depend upon the internal structure which is caused herein by using different values of μ_p during compression tests.

References

[1] P.A. Cundall, O.D.L. Strack, Geotechnique **29**, 19 (1979)
[2] C. O'Sullivan, *Particulate discrete element modelling: a geomechanics perspective* (Taylor & Francis, 2011)
[3] S. Plimpton, J. Comput. Phys. **117**, 20 (1995)
[4] J. Jaky, J. Soc. Hung. Eng. Arch **78**, 4 (1944)
[5] H.C. Nguyen, *Micromechanics of shear wave propagation and non-linear stiffness of granular materials*, PhD thesis, Imperial College London, (2020)
[6] H.C. Nguyen, M. Otsubo, C. O'Sullivan, EPJ Web of Conferences **140**, 4 (2017)
[7] H.C. Nguyen, C. O'Sullivan, M. Otsubo, Geotech. Lett. **8**, 7 (2018)
[8] J.C. Lopera Perez, C.Y. Kwok, C. O'Sullivan, X. Huang, K.J. Hanley, Geotech. Lett. **5**, 8 (2015)
[9] F.Radjai, M. Jean, J. J. Moreau, and S. Roux, Phys. Rev. Lett. **77**, 4 (1996)